Thanks for your contribution to this paper. I have read your comments very seriously and responded as follows:

Reply to the Specific comments 1: The detailed method of FRAM-SBAS technology is added in Section 3.2.2. Such as:

The main key steps of the FRAM-SBAS (Full Rank Matrix-Small Baseline Subset InSAR) method are:

Firstly, the principle of interferogram generation is based on a specific time base and space baseline, and the appropriate redundant interferogram is selected to maximize the interferogram coherence. The main constraints are

$$\left|\Delta B_{\perp}\right| < B_{\perp thr}$$

$$\left|\Delta t\right| < t_{thr}$$

$$\left|\Delta DC\right| < DC_{thr}$$

Where $\Delta B_{\perp}$ is the vertical baseline of data interference pairs, Δt is the time baseline and ΔDC is the Doppler frequency difference.

Secondly, selection of coherence points. The coherence point is selected based on the principle of full rank matrix, which effectively improves the quality of coherent point selection and provides the basis for subsequent least squares inversion. By constructing a single set interferogram network, each point can construct the following matrix (Equation 1). Where A is a $M * N$ dimensional matrix, M is the number of interferograms, and N is the number of images. For any pixel in any interferogram, the coherence is greater than a certain threshold, and the -1 and 1 flags can be set at the corresponding positions of the matrix A of Equation 1. For example, the first interferogram consists of the first image and the third image, that is $\delta_{\phi 1}=\phi_3-\phi_1$. If the interference of a certain point in the interferogram satisfies the condition, the corresponding position are $A_{11}=-1$ and $A_{13}=1$, and the remaining positions of the first line are 0. Similarly, the second interferogram, if the coherence of the point in one of the interferograms is less than the coherence threshold, the diversion is set to zero. All interferograms are judged to obtain each point pair matrix, and then the rank of each matrix is judged. If the matrix is full rank, the point is selected as the coherence point. The method can select coherent points that are coherent in the time series and coherent in the partial time interval but the interference network is connected, thereby increasing the number and precision of the coherent points.

$$A=\begin{bmatrix} -1 & 0 & 1 & \cdots & 0 & 0 & 0 \\ 0 & -1 & 1 & \cdots & 0 & 0 & 0 \\ & & \cdots\cdots\cdots & & & & \\ & & \cdots\cdots\cdots & & & & \\ 0 & 0 & 0 & \cdots & -1 & 1 & 0 \\ 0 & 0 & 0 & \cdots & -1 & 0 & 1 \end{bmatrix} \quad (1)$$

Thirdly, discrete point phase unwrapping. In the FRAM-SBAS method, discrete coherence point data is resampled onto a regular Cartesian grid, and phase unwrapping is performed using a network flow method. Then, the phase jump is checked by the closed ring residual method, and the jump phase is corrected for the jump region.

Fourthly, orbital and atmospheric error removal. The orbit error removal is performed using the network method proposed by Biggs et al., (2007). The atmospheric error is divided into long-wavelength atmospheric delay error and turbulent atmospheric delay error and terrain-related atmospheric delay error. The three errors are removed using the network methods.

Fifthly, the deformation result is obtained. The interference pattern is settled using the least squares method to obtain the deformation results of the study area.

Reply to the Specific comments 2: In Section 4.1, the comparison between the results of this paper and the results of others is added, and the reliability of the results is verified.

In this paper, the SAR data from 2003 to 2012 are analyzed. It is concluded that during the construction of the Qinghai-Tibet Railway, the linear variable along the railway is about 10mm/yr. After the completion of the traffic, the linear variable along the railway is 4~8mm/yr. Li et al., (2012) used used SBAS technology to analyze the ENVISAT ASAR data from 1997 to 2010 in the vicinity of Yangbajing-Dangxiong of Qinghai-Tibet Railway. It was found that the settlement rate near the railway was 2mm/yr, and the impact of frozen soil was about 10mm/yr. Zhang et al., (2017) used Sentinel-1 data to analyze the deformation variables of the Qinghai-Tibet Railway during the period of 2014-2016 in the Qinghai-Tibet Plateau. It is concluded that the settlement rate of the Qinghai-Tibet Railway is about -10 mm/yr and the settlement rate of the rail-stabilized area is about -5 mm/yr. Ma et al., (2011) and Dong et al., (2013) analyzed that the overall shape of the Qinghai-Tibet Railway subgrade is <10mm/yr. At the junction of the fracture, we verified it with GPS, which proves that the GPS result is highly consistent with the deformation field acquired by InSAR.

Reply to the Technical corrections 1: References and formats to the full text have been revised.

Reply to the Technical corrections 2: global positioning systems (GPS) changed into Global Positioning Systems (GPS)

Reply to the Technical corrections 3: In section 2, the corresponding references have been added.
he Qinghai-Tibet Railway is a high-elevation railway that connects Xining (Qinghai Province) to Lhasa (Tibet Autonomous Region) (Figure 1). The Qinghai-Tibet Railway and other national key projects that cross multiple active blocks and faults are vulnerable to earthquakes and other disasters (Chen et al., 2018; Wu et al., 2016). Monitoring the deformation of these projects is of great significance. InSAR and Global Positioning Systems (GPS) are efficient techniques for monitoring the crustal deformation of Qinghai-Tibet blocks (Zhang et al., 2017).
The Qinghai-Tibet Railway, highway, transmission line and other national key projects, with their ancillary studies, have the characteristics of strong correlations and continuous long-distance distributions. We need to understand how to use these features to monitor the deformation of a long linear region and reveal the movement of the Qinghai-Tibet Plateau block patterns with the deformations of these major project networks.
The Lhasa-Nagqu part of the railway is located at the bottom of the southern valley of the Nyainqentanglha Mountain in the central part of the Lhasa block (Jiang et al., 2018). In general, it is north-trending, and the Qinghai-Tibet highway and Lhasa River pass through the area. Figure 2 shows the study area, and the base map is derived from a digital elevation model (DEM). The terrain in the area is undulating, with the Nyainqentanglha Mountain Range in the northwest, a mountainous area in the southeast, and the Yangbajing-Damxung Basin in the middle of the region (Wu et al., 2018). The terrain is flat, the Qinghai-Tibet Railway and Qinghai-Tibet Highway pass through the basin, and the vegetation along the railway is rich. Wetlands and low-order regions are widely distributed, and the frozen soil in a long part of the area is rich with ice (Li et al., 2012). The study area is in a midlatitude region, and the land types mainly comprise glaciers, snow, bare rock and other land types. In this area, the Bengco fault lies across the railway; therefore, we also need to study whether the movement of the Bengco fault affects the stability of the railway.

Reply to the Technical corrections 4: The tense of Section 3.1 was modified.
The TerraSAR-X data were acquired in stripmap mode, with an incidence angle range of 39 °-40 ° at HH polarization. The potential of the X-band data for detecting higher deformation gradients compared to that of other sensors benefits from high spatial and temporal resolutions. Nevertheless, the coverage of the stripmap mode data is was too small to study long linear engineering. Therefore, in this paper, the C-band ASAR data and TerraSAR-X data were used to analyze the stability of the Qinghai-Tibet Railway. The TerraSAR-X data was selected to verify the accuracy of the ASAR T405 data results over the first corner of the railway in Yangbajain and the ASAR T133 data were used to analyze the deformation of the railway near the Nagqu area because the ASAR T405 data could not cover this area completely, and the ASAR T133 data could also verify the accuracy of the ASAR T405 data results over the Nagqu area. The data coverage was shown in Figure 2 with the blue dotted line.
The ASAR T405 data were acquired from August 2003 to September 2010, but there were no data

for 2016; therefore, we processed the data in three stages (2003-2005, 2007, and 2008-2010). The ASAR T133 data were acquired from November 2007 to August 2010. The TerraSAR-X data were acquired from December 2011 to November 2012.

Reply to the Technical corrections 5: In Figure 4,interferograms changed into interferogram.

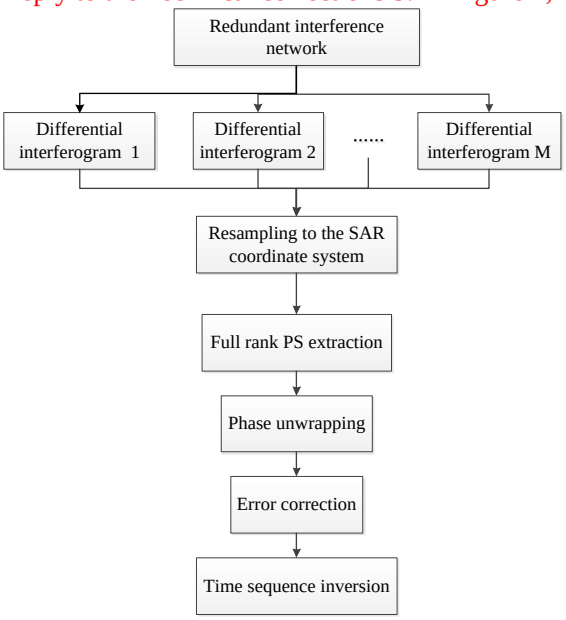

Reply to the Technical corrections 6: The Figures 5, 6 and 7 combined as figure 5.

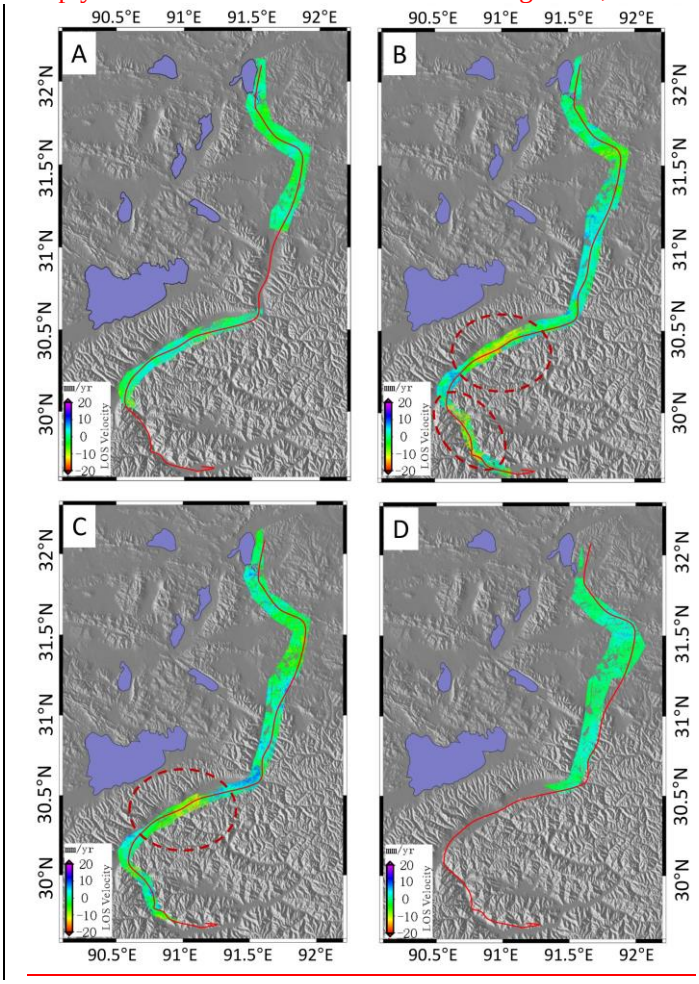

References

Chen, T., Ma, W., and Zhou, G.: Numerical analysis of ground motion characteristics in permafrost regions along the Qinghai-Tibet Railway, Cold Regions Science & Technology, 148, 88-95, https://doi.org/10.1016/j.coldregions.2018.01.016, 2018.

Dong, C. H., and Zhao, X. Q.: Analysis on subgrade deformation features and influence factors in permafrost regions on Qinghai-Tibet Railway, Railway Standard Design, 6: 5-8, 2013.

Jiang, Y., Gao, Y., Dong, Z. B., Liu, B. L., and Zhao, L.: Simulations of wind erosion along the Qinghai-Tibet Railway in north-central Tibet, Aeolian Research, 32, 192-201, https://doi.org/10.1016/j.aeolia.2018.03.006, 2018.

Li, S. S.: The study of using SBAS to monitor the Motion of the frozen soil along Qinghai-Tibet railway, Central south university, 2012

Ma, W., Liu, D., and Wu, Q. B.: Monitoring and analysis of embankment deformation in permafrost regions of Qinghai-Tibet Railway, Rock Mechanics, 29(3) : 571-580, 2008.

Ma, W., Mu, Y. H., and Wu, Q. B.: Characteristics and mechanisms of embankment deformation along the Qinghai-Tibet Railway in permafrost regions, Cold Regions Science and Technology, 67(3) : 178-186, 2011.

Wu, Z. J., Ma, W., Chen, T., and Wang, L.: Dynamic Stability Analysis of Embankment Along the Qinghai-Tibet Railroad in Permafrost Regions, Environmental Vibrations and Transportation Geodynamics, 757-766, Doi: 10.1007/978-981-10-4508-070, 2016.

Zhang, Z. J.: Research on Qinghai-Tibet Permafrost Environment and Engineering using High Resolution SAR Images, Institute of Remote Sensing and Digital Earth, Chinese Academy of Science, 2017.